the saturated behavior of the phase in the valley, our results do not agree with the recent prediction by Gerland *et al.* (*9*), who calculated the saturation of the phase to be at $\pi/2$. Although the conductance usually serves as a qualitative and approximate mark to the onset of the Kondo correlation, the phase evolution has a distinctively different and pronounced behavior in the Kondo regime. This behavior abruptly changes as the Kondo correlation weakens, evolving into the known Coulomb Blockade regime. The reasons for the deviation of the measured phase from the fundamental predictions are presently not clear. We believe that a complete insight into the Kondo-correlated regime can only be achieved after full understanding of the Coulomb Blockade regime.

References and Notes

1. J. Kondo, in *Solid State Physics*, H. Ehrenreicht, F. Seitz, D. Turnbull, Eds. (Academic Press, New York, 1969), vol. 23, pp. 183–281.
2. P. W. Anderson, *Phys. Rev.* **124**, 41 (1961).
3. L. I. Glazman, M. E. Raikh, *JETP Lett.* **47**, 452 (1988).
4. T. K. Ng, P. A. Lee, *Phys. Rev. Lett.* **61**, 1768 (1988).
5. U. Meirav, E. B. Foxman, *Semicond. Sci. Technol.* **10**, 255 (1995).
6. D. Goldhaber-Gordon *et al.*, *Nature* **391**, 156 (1998).
7. D. C. Langreth, *Phys. Rev.* **150**, 516 (1966).
8. P. A. Nozieres, *J. Low Temp. Phys.* **17**, 31 (1974).
9. U. Gerland, J. von Delft, T. A. Costi, Y. Oreg, *Phys. Rev. Lett.* **84**, 3710 (2000).
10. A. Yacoby, M. Heiblum, D. Mahalu, H. Shtrikman, *Phys. Rev. Lett.* **74**, 4047 (1995).
11. R. Schuster *et al.*, *Nature* **385**, 417 (1997).
12. Y. Meir, N. S. Wingreen, P. A. Lee, *Phys. Rev. Lett.* **70**, 2601 (1993).
13. N. S. Wingreen, Y. Meir, *Phys. Rev. B* **49**, 11040 (1994).
14. J. Schmid, J. Weis, K. Eberl, K. von Klitzing, *Phys. Rev. Lett.* **84**, 5824 (2000).

15. We thank D. Goldhaber-Gordon and E. Buks for valuable suggestions on the fabrication process and measurement techniques. We also thank J. von Delft and Y. Oreg for helpful discussions before publication. Supported in part by the MINERVA foundation.

21 July 2000; accepted 20 September 2000

Moissanite: A Window for High-Pressure Experiments

Ji-an Xu and Ho-kwang Mao

We achieved a pressure of 52.1 gigapascals with moissanite anvils, which have optical, thermal, electric, magnetic, and x-ray properties that rival those of diamond. The mode-softening of D_2O toward the pressure-induced hydrogen bond symmetrization and the Raman shifts of diamond under hydrostatic and nonhydrostatic compressions were studied with moissanite anvils in the spectral regions normally obscured by diamond anvils. Moissanite anvil cells allow maximum sample volumes 1000 times larger than those allowed by diamond anvil cells and may enable the next level of advancement in high-pressure experiments.

Sustained breakthroughs in ultrahigh-pressure technology over the past 25 years have had impacts in areas ranging from fundamental physics and chemistry (*1*, *2*) to earth, planetary (*3*), and materials research (*4*). Pressures achievable with the Mao-Bell–type diamond anvil cell (DAC) exceeded the 50-GPa (half-megabar) barrier in 1975 (*5*) and subsequently increased to hundreds of GPa (*6–9*). The DAC thus became the only research tool for static pressure experiments above 30 GPa. The infrared, visible, x-ray transparency, and other favorable properties of diamond provide a window for laser (*10*), x-ray (*11*, *12*), electric (*13*), and magnetic (*14*) microprobes in situ at high pressures. The use of diamonds, however, also imposes limitations. The characteristic infrared, Raman, and Brillouin peaks of diamond interfere with measurements of sample peaks in similar spectral regions. Diamond shows surface oxidation above 900 K and burns above 1120 K in air and must be kept in a reducing atmosphere for experiments at high pressure and temperature (*P-T*) with external heating (*15*). The most severe constraint is that perfect diamonds have limited availability and very high cost, restricting high-pressure samples to microscopic volumes (10^{-10} to 10^{-13} liters).

Previous experiments in the search for superhard gem anvils to use as replacements or complements for diamond have only reached pressures of a maximum of 16.7 GPa with cubic zirconia (*16*) and 25.8 GPa with sapphire (*17*). With a hardness (Knoop scale) of 3000, synthetic moissanite (hexagonal silicon carbide) is harder than sapphire (2000) and cubic zirconia (1370) but softer than diamond (5700 to 10,400). Large, gem-quality, single-crystal moissanite has recently become available (*18*). We carried out experiments using moissanite anvils with the *c* crystallographic direction parallel to the compression axis. The fluorescence spectra of ruby grains compressed without a pressure medium were measured through the moissanite window for pressure calibration (Fig. 1). The moissanite anvils readily achieved 52.1 GPa.

Complementary to diamond, moissanite provides a clear window between 0.4 and 5.5 μm for optical spectroscopy. For instance, moissanite has sharp Raman spectral peaks at 149.6, 766.9, 788.4, and 964.7 cm^{-1} that do not overlap with the first-order Raman peak of diamond at ν_0 = 1333 cm^{-1} or with the broad multiphonon second-order Raman band of diamond in the region from 2300 to 2700 cm^{-1}. High-pressure phase transitions and symmetrization of hydrogen bonds in H_2O and D_2O ices have been characterized by Raman mode-softening (*19–21*). With moissanite anvils, we observed the evolution and splitting of E_g and B_{1g} peaks of D_2O ices in the spectral region from 2300 to 2700 cm^{-1} without the background interference of diamond anvils (Fig. 2).

A fundamental problem for understanding the bonding nature of superhard materials is the effect of hydrostatic and nonhydrostatic stresses on the first-order Raman peak of diamond itself (*22–24*). Separation of the Raman peaks of the diamond samples and the DAC is difficult, particularly at pressures below 10 GPa, when the total shift is less than the bandwidth of the peaks. Isotopic ^{13}C-

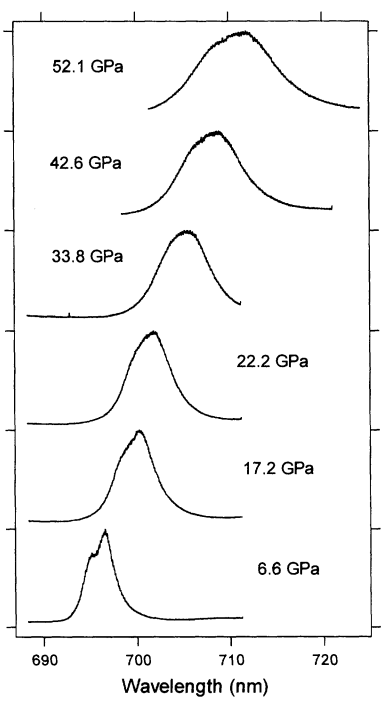

Fig. 1. Ruby fluorescence spectra observed in a MAC up to 52.1 GPa. The experiments were conducted with a moissanite anvil with a 300-μm-diameter flat culet opposing a second anvil with a 300-μm 10° beveled culet with a 100-μm central flat culet.

Center for High Pressure Research and Geophysical Laboratory, Carnegie Institution of Washington, 5251 Broad Branch Road, NW, Washington, DC 20015, USA.

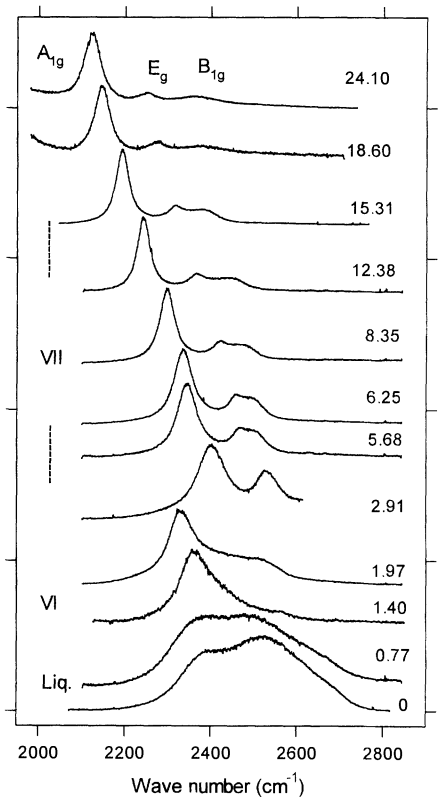

Fig. 2. High-pressure Raman spectra of liquid D_2O (0 and 0.77 GPa), ice VI D_2O (1.40 and 1.97 GPa), and ice VII D_2O (≥2.91 GPa), measured in a MAC at 298 K.

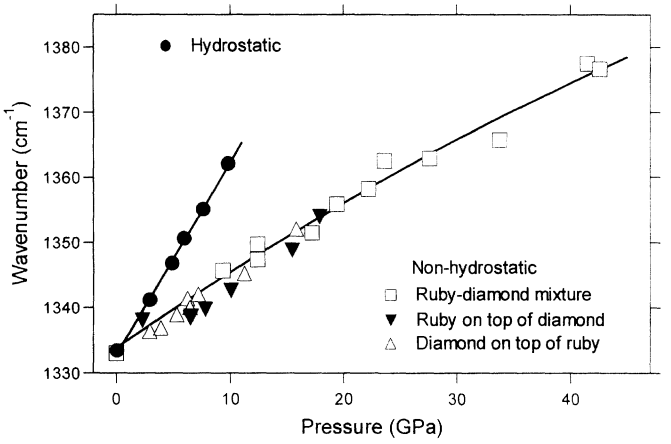

Fig. 3. First-order Raman frequency shift of diamond samples as a function of hydrostatic (in an ethanol-methanol pressure medium) (circles) and nonhydrostatic (without a pressure medium) compressions in a MAC. Three different nonhydrostatic sample configurations yielded similar results: squares, mixture of ruby and diamond powder; solid triangles, ruby powder sprinkled on top of compacted diamond powder; open triangles, diamond powder sprinkled on top of compacted ruby powder.

enriched diamond samples have been used for the peak separation, but the pressure coefficients of the ^{13}C and ^{12}C diamonds are different (*24*). We used a moissanite anvil cell (MAC) to overcome the problem and observed a pressure shift of $\partial\upsilon/\partial P = 2.96 \pm 0.05$ cm^{-1} GPa^{-1} for the natural diamond sample compressed in a hydrostatic medium up to 10 GPa (Fig. 3). This is in good agreement with the highest reported value of 2.93 cm^{-1} GPa^{-1} (*23*) measured above 10 GPa in a helium pressure medium in a DAC, indicating that previously reported lower values [see summary in (*24*)] are contaminated by the spectra of DACs or caused by various degrees of nonhydrostaticity in the sample. We also studied diamond Raman peaks under the maximum nonhydrostatic stress in a MAC and observed much smaller peak shifts ($\partial\upsilon/\partial P = 1.0 \pm 0.1$ cm^{-1} GPa^{-1}), about one-third of the hydrostatic value (Fig. 3). The triple degeneracy of the F_{2g} zone center phonon is lifted in the randomly oriented diamond grains under nonhydrostatic compression, resulting in a broad peak that would be completely obscured by the DAC but is visible in the Raman spectrum obtained with the MAC. With the complementariness of diamond and moissanite, the entire ultraviolet-visible-infrared spectral range from 200 nm to 200 μm can now be explored with Raman, Brillouin (*25*), absorption, reflectance, and other spectroscopies, free of anvil interference.

With its high thermal conductivity (500 W m^{-1} K^{-1} at 293 K) and transparency in the near-infrared, moissanite behaved similarly to diamond when tested by double-sided Nd:yttrium-aluminum-garnet laser heating to 3700 K at 3 GPa of a graphite sample sandwiched between two layers of NaCl platelets. We also heated moissanite anvils in air to 1400 K for 36 hours without damage, showing that the moissanite anvil is useful for high *P-T* experiments with resistive heating. Like diamond (*26*), moissanite anvils have been used to seal and solidify the hard-to-contain hydrogen and helium gases. Moissanite is a wide-gap insulator suitable for high-pressure electric conductivity measurements (*13*) and has no detectable magnetic signal to interfere with high-pressure magnetic measurements (*14*). Moissanite is a strong x-ray absorber below 20 keV and is thus unsuitable for x-ray diffraction with the conventional Mo Kα source, but is transparent at x-ray energies above 25 keV, which is the main region for high-pressure synchrotron experimentation with monochromatic x-radiation. We have obtained energy-dispersive x-ray diffraction patterns of graphite samples in MACs that are comparable to DAC results above 25 keV. Moissanite is amenable to shaping by diamond tools and opens new possibilities for intricate anvil configurations.

Finite-element calculations (*27*) have demonstrated that, within the strength limitations of the anvil materials, larger sample volumes can be used at the same maximum pressures by proportionally scaling up the dimensions of the anvils, gaskets, and samples. We have verified this conclusion experimentally with diamond anvils ranging from 0.02 to 2 carats. Single-crystal moissanite is available up to the volume equivalent of a 300-carat diamond anvil. Scaling up the MAC design with such large moissanite anvils will be suitable for compressing millimeter-sized samples to 50 GPa and will allow sample volumes 1000 times greater than with a typical DAC, which has <0.3 carat of diamond. The large sample size could allow the use of additional types of analysis, such as neutron diffraction (*28*), neutron scattering (*29*), inelastic x-ray spectroscopy, x-ray Compton scattering, nuclear magnetic resonance (*30*), and ultrasonic interferometry (*31*, *32*). The larger sample could also improve the currently established techniques, including x-ray diffraction, optical spectroscopy, electric conductivity (*13*), and magnetic susceptibility (*14*).

References and Notes

1. R. J. Hemley, N. W. Ashcroft, *Phys. Today* **51**, 26 (1998).
2. V. Iota, C. S. Yoo, H. Cynn, *Science* **283**, 1510 (1999).
3. R. J. Hemley, *Science* **285**, 1026 (1999).
4. P. F. McMillan, *Nature* **391**, 539 (1998).
5. H. K. Mao, P. M. Bell, *Carnegie Inst. Wash. Year Book* **74**, 402 (1975).
6. ———, *Science* **191**, 851 (1976).
7. ———, *Science* **200**, 1145 (1978).
8. P. M. Bell, H. K. Mao, K. Goettel, *Science* **226**, 542 (1984).
9. J. Xu, H. K. Mao, P. M. Bell, *Science* **232**, 1404 (1986).
10. R. J. Hemley, P. M. Bell, H. K. Mao, *Science* **237**, 605 (1987).
11. T. Takahashi, W. A. Bassett, *Science* **145**, 483 (1964).
12. R. J. Hemley *et al.*, *Science* **276**, 1242 (1997).
13. M. I. Eremets, K. Shimizu, T. C. Kobayashi, K. Amaya, *Science* **281**, 1333 (1998).
14. V. V. Struzhkin, R. J. Hemley, H. K. Mao, Y. A. Timofeev, *Nature* **390**, 382 (1997).
15. Y. Fei, H. K. Mao, *Science* **266**, 1678 (1994).
16. J. Xu, S. Yeh, J. Yen, E. Huang, *J. Raman Spectrosc.* **27**, 823 (1996).
17. J. Xu, J. Yen, Y. Wang, E. Huang, *High Pressure Res.* **15**, 127 (1996).
18. K. Nassau, S. F. McClure, S. Elen, J. E. Shigley, *Gems Gemol.* **33**, 260 (1997).
19. P. Pruzan, J. C. Chervin, M. Gauthier, *Europhys. Lett.* **13**, 81 (1990).
20. A. F. Goncharov, V. V. Struzhkin, M. Somayazulu, R. J. Hemley, H. K. Mao, *Science* **273**, 218 (1996).
21. A. F. Goncharov, V. V. Struzhkin, H. K. Mao, R. J. Hemley, *Phys. Rev. Lett.* **83**, 1998 (1999).

22. M. Hanfland, K. Syassen, S. Fahy, S. G. Louie, M. L. Cohen, *Phys. Rev. B* **31**, 6896 (1985).
23. I. V. Aleksandrov, A. F. Goncharov, A. N. Zisman, S. M. Stishov, *Sov. Phys. J. Exp. Theor. Phys. Lett.* **66**, 384 (1987).
24. D. Schiferl *et al.*, *J. Appl. Phys.* **82**, 3256 (1997).
25. T. S. Duffy, W. L. Vos, C.-S. Zha, R. J. Hemley, H. K. Mao, *Science* **263**, 1590 (1994).
26. H. K. Mao, P. M. Bell, *Science* **203**, 1004 (1979).
27. S. Merkel, R. J. Hemley, H. K. Mao, *Appl. Phys. Lett.* **74**, 656 (1999).
28. R. J. Nelmes *et al.*, *Phys. Rev. Lett.* **81**, 2719 (1998).
29. P. Link, I. N. Goncharenko, J. M. Mignot, T. Matsumura, T. Suzuki, *Phys. Rev. Lett.* **80**, 173 (1998).
30. S. H. Lee, M. S. Conradi, R. E. Norberg, *Rev. Sci. Instrum.* **63**, 3674 (1992).
31. W. A. Bassett *et al.*, in *Proceedings of International Conference AIRAPT-16 and HPCJ-38 on High Pressure Science and Technology*, vol. 7 of *The Review of High Pressure Science and Technology* (Japan Society of High Pressure Science and Technology, Kyoto, 1998), pp. 142–144.
32. B. Li, R. C. Liebermann, D. J. Weidner, *Science* **281**, 675 (1998).
33. Supported by the Center for High Pressure Research grant of NSF.

26 July 2000; accepted 19 September 2000

Förster Energy Transfer in an Optical Microcavity

Piers Andrew* and William L. Barnes

By studying the transfer of excitation energy between dye molecules confined within an optical microcavity, we demonstrate experimentally that Förster energy transfer is influenced by the local photonic mode density. Locating donor and acceptor molecules at well-defined positions allows the transfer rate to be determined as a function of both mutual separation and cavity length. The results show that the Förster transfer rate depends linearly on the donor emission rate and hence photonic mode density, providing the potential to control energy transfer by modification of the optical environment.

Processes involving the interaction between light and matter are fundamental to much of science. An important example is the transfer of excitation energy from an excited donor molecule to an acceptor molecule through the resonant dipole-dipole interaction (RDDI). In addition to its key role in photosynthesis (*1*, *2*), this process is of increasing importance as a means of improving the functionality and efficiency of light-emitting diodes and lasers based on organic materials (*3*, *4*). Control of the spontaneous emission of light is accomplished by the use of structures in which the photonic mode density (PMD) is altered, thus manipulating the optical modes into which emission may take place (*5*, *6*). A wealth of research based on this concept is found within the areas of cavity quantum electrodynamics (*7*) and photonic band gap materials (*8*), and it would be of great interest if one could similarly enhance energy transfer. Here, we demonstrate that such enhancement is possible for the Förster transfer process by studying the transfer of excitation energy between molecules confined within an optical microcavity.

The physical nature of the excitation energy transfer mechanism depends on the donor-acceptor separation, d. When the donor and acceptor are far apart ($d > \lambda/10$), transfer is radiative, coupling being mediated by a real photon. In contrast, when donor and acceptor are close, transfer is nonradiative, being mediated by a virtual photon, a process known as Förster transfer (*9*). Both processes involve interactions between the dipole moments of the donor and acceptor molecules (*10*); the radiative process proceeds through the dipole far field, whereas nonradiative transfer occurs through the evanescent near-field components.

Various theoretical investigations have examined how the RDDI is modified by confined geometries such as microcavities (*11*–*13*) and periodic structures (*14*, *15*). They predict that the PMD affects the RDDI, the strength of the effect dependent on the donor-acceptor separation. Recent experiments on microcavities containing donors and acceptors in well-defined and widely separated positions ($\sim\lambda/4$) have demonstrated control over the radiative transfer process (*16*). To investigate the nonradiative Förster process requires a much reduced separation between donor and acceptor molecules. Hopmeier *et al.* (*17*) studied transfer between donors and acceptors randomly distributed throughout a cavity, observing increased acceptor emission when the transfer energy was resonant with a cavity mode. However, because Förster transfer depends strongly on the donor-acceptor separation, they were unable to draw any conclusions about the influence of the cavity on the nonradiative transfer process. The absence of appropriate experimental information leaves open the question of whether Förster transfer can be controlled by the local optical environment.

To explore this question, we measured energy transfer between monomolecular layers of donor and acceptor molecules separated by known distances contained within a series of microcavity structures. Locating donors and acceptors at fixed positions within the microcavity structure ensured that the molecules experienced the same PMD. We show that transfer is by the Förster process and that the transfer rate depends on the PMD, demonstrating that modification of the local optical environment can be used to control the Förster transfer process.

The length scale associated with the Förster process is called the critical distance and corresponds to the donor-acceptor separation for which the transfer rate equals the sum of all other donor decay rates, of order 5 nm. Because of this small characteristic distance, we need molecular resolution in the position of the donor and acceptor molecules, which we achieved using the Langmuir-Blodgett technique. This monomolecular deposition technique allows fabrication of microcavities in which cavity length, donor-acceptor separation, and position within the cavity can be specified with molecular precision. To clarify the effect of PMD on Förster transfer, we used a donor with monochromatic emission, ensuring a single transfer wavelength. This was achieved by the use of a Eu^{3+} complex [*N*-hexadecyl pyridinium tetrakis (1,3-diphenyl-1,3-propandionato) europium (III)] as the donor molecule because the electric dipole transition at 614 nm has a width of only ~5 nm and the long lifetime (~1 ms) allows accurate dynamic measurements of the transfer process. The acceptor, 1,1′-dioctadecyl-3,3,3′,3′-tetramethylindodicarbocyanine, has a high absorption coefficient at the donor emission wavelength, allowing very efficient transfer to take place. The relevant absorption and emission spectra are given in Fig. 1. The combination of high absorption and excellent spectral overlap results in an extremely large critical transfer distance (~14 nm), ensuring that we can measure the distance dependence of the transfer with sufficient spatial resolution by intercalation of monomolecular spacer layers (thickness = 2.6 nm) between donor and acceptor layers.

The energy transfer system that we used consisted of donor and acceptor monolayers separated by zero, two, four, six, and eight layers, respectively, of a transparent material, 22-tricosenoic acid. The strong distance dependence of the Förster process means that transfer from the donor occurs predominantly to the nearest acceptor. To ensure that the donor–nearest acceptor separation coincided with the donor-acceptor layer separation, we had to use highly condensed acceptor monolayers (area per molecule ~1 nm^2). In this way, we could vary the separation between donors and acceptors from 0 to 25 nm in a carefully controlled manner. A consequence of the highly condensed acceptor layer is that the acceptor emission is strongly self quenched and we were

Thin Film Photonics Group, School of Physics, University of Exeter, Exeter, EX4 4QL, UK.

*To whom correspondence should be addressed. E-mail: pandrew@exeter.ac.uk